

PermeabilityNets: comparing neural network architectures on a sequence-to-instance task in CFRP manufacturing

Simon Stieber, Niklas Schroter, Ewald Fauster, Alexander Schiendorfer, Wolfgang Reif

Angaben zur Veröffentlichung / Publication details:

Stieber, Simon, Niklas Schroter, Ewald Fauster, Alexander Schiendorfer, and Wolfgang Reif. 2021. "PermeabilityNets: comparing neural network architectures on a sequence-to-instance task in CFRP manufacturing." In *2021 20th IEEE International Conference on Machine Learning and Applications (ICMLA), Pasadena, CA, USA, 13-16 December 2021*, edited by M. Arif Wani, Ishwar Sethi, Weisong Shi, Guangzhi Qu, Daniela Stan Raicu, and Ruoming Jin, 694–97. Piscataway, NJ: IEEE.
<https://doi.org/10.1109/icmla52953.2021.00116>.

Nutzungsbedingungen / Terms of use:

licgercopyright

Dieses Dokument wird unter folgenden Bedingungen zur Verfügung gestellt: / This document is made available under these conditions:

Deutsches Urheberrecht

Weitere Informationen finden Sie unter: / For more information see:

<https://www.uni-augsburg.de/de/organisation/bibliothek/publizieren-zitieren-archivieren/publiz/>



PermeabilityNets: Comparing Neural Network Architectures on a Sequence-to-Instance Task in CFRP Manufacturing

Simon Stieber*, Niklas Schröter*, Ewald Fauster[†], Alexander Schiendorfer*[‡], Wolfgang Reif*

*Institute for Software & Systems Engineering, University of Augsburg, Augsburg, Germany

Email: {stieber, schroeter, reif}@isse.de

[†]Processing of Composites Group, Montanuniversität Leoben, Austria

Email: Ewald.Fauster@unileoben.ac.at

[‡]Digital Production Group, Technische Hochschule Ingolstadt, Germany

Email: Alexander.Schiendorfer@thi.de

Abstract—Carbon fiber reinforced polymers (CFRP) offer highly desirable properties such as weight-specific strength and stiffness. Liquid composite moulding (LCM) processes are prominent, economically efficient, out-of-autoclave manufacturing techniques and, in particular, resin transfer moulding (RTM), allows for a high level of automation. There, fibrous preforms are impregnated by a viscous polymer matrix in a closed mould. Impregnation quality is of crucial importance for the final part quality and is dominated by preform permeability. We propose to learn a map of permeability deviations based on a sequence of camera images acquired in flow experiments. Several ML models are investigated for this task, among which ConvLSTM networks achieve an accuracy of up to 96.56%, showing better performance than the Transformer or pure CNNs. Finally, we demonstrate that models, trained purely on simulated data, achieve qualitatively good results on real data.

I. RTM AND PERMEABILITY MEASUREMENTS

Carbon fiber reinforced polymers (CFRP) are superior to other engineering materials in terms of weight-specific mechanical properties such as strength and stiffness. Replacing conventional steel or aluminum with CFRP helps reduce fuel consumption and CO₂ emissions. These composite materials are made from a polymer matrix that is reinforced with fibers made from carbon. To produce CFRP parts industrially, liquid composite moulding (LCM) processes are one of the most prominent, economically efficient out-of-autoclave manufacturing techniques. More specifically, resin transfer molding (RTM, [1]) is a commonly applied manufacturing process for medium volumes (1,000s to 10,000s of parts per year): A liquid thermoset polymer (called a resin) is injected under pressure into a mold cavity that contains the reinforcement material, i.e., a textile of carbon fibers (called the preform). During injection, this results in a “flow front” that separates impregnated material from dry material (cf. Fig. 2).

This research is funded by the Bavarian Ministry of Economic Affairs, Regional Development and Energy in the project CosiMo.

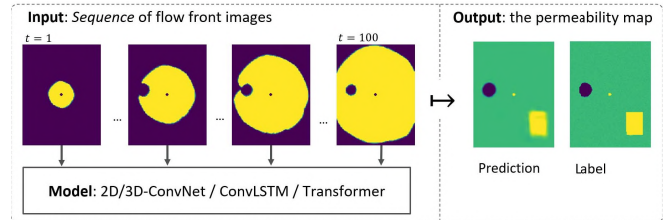


Fig. 1. Overview of the sequence-to-instance learning task: a sequence of flow front images is mapped to an image that contains the permeability values of the material, i.e., the permeability map.

The temporal progress of the flow front is predominantly influenced by the *permeability* characteristics of the preform, which describes the ability of a porous medium to transmit fluids. In CFRP, the preform permeability is dominated by (i) fiber volume content (FVC) and (ii) preform architecture. Local changes of preform permeability can occur at curved sections of the component or at locations of wall thickness changes. In addition, they may be caused by imperfect material properties (e.g., missing or misaligned fiber bundles) or by manual handling of the fibrous structure. The variation of permeability can reach up to 20% [2]. Local variations in permeability affect the temporal progress of the flow front and can thus cause suboptimal impregnation quality or even dry spots, deteriorating the mechanical performance. These variations are typically unknown for an individual preform prior to or during an industrial RTM process – a map of FVC or permeability values would be highly desirable to diagnose issues early on. Equipping the mold with sensors facilitates in-situ monitoring of the injection process [3].

Aside from industrial RTM instances, permeability characteristics of preform materials can be experimentally determined by means of permeability characterization cells, as shown in Fig. 2. For the study at hand, an 2-D in-plane, optical permeability characterization cell (called a *permeameter*) was

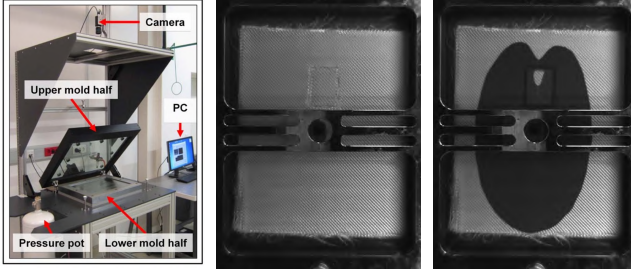


Fig. 2. Permeameter experiments: Left: In-plane permeameter system with an optically transparent upper mould half. Middle: Beginning of injection trial in permeameter, a dark spot is visible between the frame. Right: the injection is in progress, with a visible deviation of the flow front caused by the patch with changed permeability, which is visible on both images.

used, which follows the radial flow technique combined with optical flow front tracking. Using an optical permeameter offers the advantage that almost the entire flow front can be tracked in the form of planar *images* instead of sensory time series at certain locations only.

Therefore, we propose to use machine learning (ML) models that predict *changes in the permeability*, given an observed *sequence of flow front images* during an injection process in a permeameter, i.e., a *sequence-to-instance task* (cf. Fig. 1). The training data is obtained from PAM RTM, an industrially applied FEM simulation tool for RTM processes (see Section II). This task constitutes a part of a larger pipeline that eventually leads to a permeability map prediction from in-mold sensory data. For that, an intermediary step that maps *sensors to flow front images* would be necessary: e.g. using transposed convolutions [3] or other generative models. To sum up, our *contributions* are: We compare several ML models for this sequence-to-instance task in an engineering domain. We apply these networks, trained on simulated data only, also on real permeameter data and demonstrate that they are able to reliably predict permeability deviations. This approach can be seen as a part of a digital twin of the process [4]. If the component does not show excessive variations in permeability and, consequently, in FVC, it can be considered acceptable.

A. Related work

The online measurement of the permeability or its deviation has received attention in the composites processing literature. Barkoula et al. [5] estimate global and local permeability during the injection with pressure and flow front sensors by calculating it with Darcy's law [6]:

$$\mathbf{v} = -\frac{1}{\eta} \mathbf{K} \nabla p, \quad (1)$$

with volume-average flow velocity \mathbf{v} , fluid viscosity η , permeability tensor \mathbf{K} and pressure drop ∇p . Darcy's law is central to liquid composite molding simulation. For 2-dimensional flow (as addressed in the work at hand), the planar, anisotropic permeability tensor is set up as follows:

$$\mathbf{K}_{2D, \text{aniso}} = \begin{bmatrix} k_x & k_{xy} \\ k_{xy} & k_y \end{bmatrix} \quad (2)$$

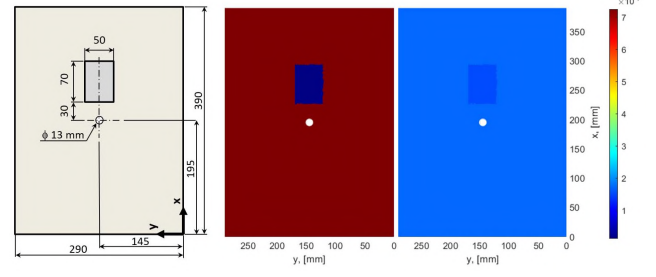


Fig. 3. Left: Measures of the final setup for the injection trials. Middle: projected k_x , Right: projected k_y (from simulation).

The permeability x and y direction is shown by k_x and k_y , whereas k_{xy} describes the dependency of the flow in one main direction on a pressure gradient in the other main direction. Gonzales et al. [7] used CNNs to detect changes in the flow front from pressure sensors to be able to detect changes in permeability. They use the data of whole recorded runs, but can only detect single, rectangular changes in permeability. Our approach is more versatile by not only detecting fixed features of the patch (such as length, width or center point) but constructing the entire permeability map of the preform. Besides online permeability estimation, other papers combine RTM analysis and ML: Stieber et al. [3] present a learning-based dry spot classifier, working only on simulated data.

II. DATA REGIME

The available data either stem from FEM-based RTM-simulations or the optical permeameters depicted in Fig. 2.

a) *Simulated data*: To obtain the *simulated data*, we followed a setup comparable to [3]: On a 2D plate of homogeneous material, we randomly inserted small patches of changed permeability and FVC into the textile of a simulated RTM process within an automated pipeline (cf. “label” in Fig. 1). These modified permeability maps provoke altered flow fronts and need to be re-discovered by the ML models. As input, the models get a sequence of flow front images, as shown in Fig. 1. We only predict the k_x permeability (as a first feasibility check of this approach), for k_y the models would need to be retrained with an additional output, k_{xy} is 0 in the simulation. A total of 10,990 runs was produced.

b) *Real data from permeameter*: To generate the real data, we introduced one patch of lower permeability at the same spot to each of six runs in the permeameter (cf. Fig. 2). To ensure that we use a patch of sufficient size and FVC to actually provoke a dry spot, we simulated different patch configurations, Fig. 3 shows the final measures. The experiments were run with a glass fiber woven fabric, type Hexion 1202 of Hexcel. Table I lists the most relevant properties of the preform in both the neat and the patch region. The reinforcing material used for the experiments in this paper shows principal flow directions well aligned with the directions of the woven fiber bundles, i.e.: $k_{xy} \approx 0$. Moreover, standard plant oil was used as a test fluid for the experiments. It exhibits a viscosity

TABLE I
PREFORM SETUP FOR REAL WORLD TRIALS

Region	# of layers	FVC	k_x [mm^2]	k_y [mm^2]
Preform mat.	11	41.7 %	72.47e-6	17.21e-6
Patch region	16	60.7 %	1.19e-6	15.32e-6

of 65 mPas at room temperature and was colored with a red color pigment to enhance image contrast of saturated preform regions against unsaturated preform regions.

To use the experimental data, especially passing it through a model trained on simulation-only data, the acquired sequence images had to be preprocessed. We transformed the permeameter images to align them with the images created by the simulation: We removed the empty area around the textile, removed the stiffening frame and approximated the parts of the image that were covered by the stiffening frame. This is done by fitting an elliptical geometry model to selected sets of flow front data [8]. After these processing steps, the approach is identical to the simulated data; the image sequences are sampled over the filling percentage of the visible flow front, while adding padding to create sequences of the same length.

We conclude the section on data by noting that creating real-world experiments is costly in a lab or in an industrial environment and thus limited data are available. Further, some fixed preprocessing necessary is required to align real images with simulated ones, e.g., due to the stabilising metal frame. While there is no measured permeability map of the real injection experiments, we can rely on the simulation permeability maps that were implemented using well-defined glass fiber woven fabrics for our evaluations in Section IV-A2.

III. APPROACH - MODEL COMPARISON

Several models are suitable to address our sequence-to-instance task. The first model we employed is a basic convolutional neural network (CNN) with four `conv2D` layers. From a subsampling step, we get 100 single-channel images of the time steps of the injection process. Since 2D convolutions work over any number of channels, we use the 100 time steps as independent channels for the first convolutional layer. The second approach emphasizes the temporal aspect by using a Convolutional Long Short Term Memory (ConvLSTM) architecture [9]. In contrast to regular LSTMs, ConvLSTMs work over sequences of two dimensional matrices, instead of one dimensional vectors, which makes them suitable for our task. The last proposed model relies on the transformer mechanism [10] which works on one-dimensional embeddings. Hence, the input image sequence needs to be converted into an embedding sequence. To do so, a fully convolutional encoder creates feature vectors for the individual images and is trained end-to-end in the sequence-to-instance pipeline. The transformer output creates the permeability map using 2D transposed convolutions. For further details, see the code¹.

¹We published the code, data and checkpoints: <https://github.com/isse-augsburg/PermeabilityNets>

TABLE II
RESULTS OVERVIEW - MODEL COMPARISON. TRAIN. TIME: ONE EPOCH

Model	IOU	Acc.	Train. time	Inf. time	Real data perf.
CNN	0.6277	94.74	52 s	24 s	**
ConvLSTM	0.7496	96.56	27:30 m	40 s	***
Transformer	0.6373	95.08	1:45 m	27 s	*

IV. EVALUATION

To evaluate our models, we had to define a set of *metrics* aside from the “expert eye” that solely investigates the output images. Defining a metric faithful to the observed performance (cf. Figure 4) turned out to be more difficult than expected since, e.g., *pixelwise accuracy* tends to focus too much on “blurry” predictions. *Exact* accuracy further proved to be uninformative due to large portions of the permeability maps having roughly similar base permeabilities. We therefore allowed ε -tolerances to still classify individual pixels as correct. On normalised images (between 0 and 1), we empirically determined ε to be 0.03 by manually inspecting prediction-label pairs. Values greater than 3% decrease the sensibility of the metric, while values smaller than 3% are too sensitive to create comparable results. In addition, we employed the *intersection over union* (IOU). This metric focuses on the extent of the detected variation in permeability and ignores the absolute value of the variation. Table II shows that the CNN and the Transformer network are the fastest models for training and inference. Certainly, the importance of speed is debatable, given the excellent performance of the slowest network, the ConvLSTM, which is further discussed in Section IV-A. The most interesting finding here is that in our case study, the Transformer shows promising results, given their short training time – albeit not outperforming the more conventional ConvLSTM. Regarding the evaluation on real data, Section IV-A2 gives a detailed insight, where the performance of the Transformer is much worse than on simulation-only data.

A. Results

1) *Sim-only*: Table II presents an overview on how each of the models performed. The ConvLSTM outperforms all other models in both IOU and accuracy. But it also takes the longest to train. The CNN model offers a reasonable tradeoff between training speed, ease of development, and quality for our problem. The Transformer gives a two-sided impression: the metrics on simulated data are close to the best models and it has very short training times, but the performance on real data is poor, as described in Section IV-A2.

Figure 4 displays the qualitative performances of the different models on selected exemplary runs². Here, the background in green shows the same base permeability, whereas higher permeability is depicted in yellow, and lower permeability is

²More examples at: <https://figshare.com/s/1d0ac937e739620fad9>

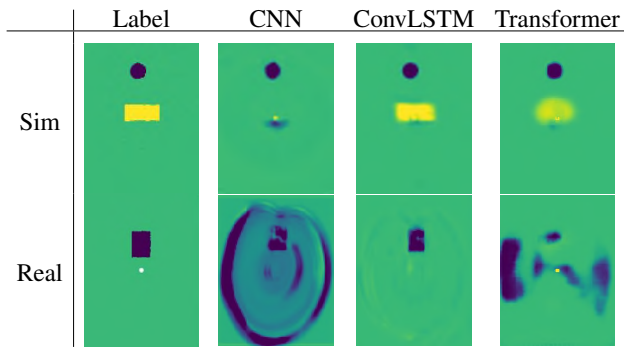


Fig. 4. Example outputs of different models on simulated and real data. Real data “labels” are taken from simulation.

shown in dark blue. The winner is again the ConvLSTM, with Transformer as the runner-up. In run *Sim*, the ConvLSTM shows the ability to detect higher permeabilities. Only the Transformer is able detect the area of higher permeability as well, but in a more blurry fashion. To sum up, the ConvNet networks performs worse than ConvLSTM and Transformer, which matches the numbers from Table II.

2) *Real data as test set - qualitative comparison of outcomes*: We do not claim to measure absolute values of the permeability during the process, but only relative changes to the permeability. Thus, we used our models, trained on simulated data, on the same task with real data from the permeameter: showing relative changes to the permeability. Figure 4 shows the result for one run for the different models. Since we do not have the measured permeability map in real life to serve as a label, we have to use the permeability map from simulation, presented in the setup in Fig. 3, for qualitative comparison. When inspecting Fig. 4, several aspects stand out directly. The qualitative performance is rated with stars in Table II. (1) The ConvLSTM outperforms every other approach by far, for every run. The patches of lower permeability have relatively clear borders and show the same, darker color, referring to lower permeability, as expected. Other than that, the rest of the textile is fairly homogeneous, with some slight artifacts, resembling the flow front (3/3 stars). (2) For the CNN, these artifacts are much stronger. When taking a closer look at these related approaches, we can observe stronger deviations for the CNN model, especially for run *Real*, while the other two show acceptable or even good results for both patch and base permeability. The CNN receives 2/3 stars. (3) Lastly, the Transformer performs the worst, by far. The outputs on the different runs look very much alike, with patches of lower permeability at all places, but the correct one. There are even slightly lighter spots at the locations, above the center, where darker patches (of lower permeability) should be for all runs. This unsatisfying performance on real data of the pretrained Transformer is an interesting result. Despite their recent popularity, for our case study, ConvLSTMs are the most accurate model and standard CNNs are also more desirable. Given the Transformer’s performance on simulated data (there, second best), these results were rather disappointing, resulting

in the lowest rating of 1 star.

V. DISCUSSION AND FUTURE WORK

As already mentioned in Section I, in-situ sensor data would be necessary to apply the results of this paper to an industrial setting. Another step would be using more real data. With that, we could try real transfer learning from simulation to reality, not just testing on real data in order to capture real-life effects that are not properly captured by simulations mainly based on Darcy’s law. We could try to learn these effects from real data and become more accurate than the simulation. Examples of these effects are channels in the textile that lead to race tracking, the faster advancement of resin at certain places, and general divergence regarding timing.

VI. CONCLUSION

We presented a comparison of three network architectures on a sequence-to-instance task in an engineering domain. This approach is geared towards a digital twin of the injection process for CFRP. Models were trained to predict permeability deviation maps from flow front image sequences. The models trained on simulated data performed well on real data stemming from a permeameter. Depending on the available training time, CNNs and ConvLSTMs showed the most promising results both on simulated and real data.

REFERENCES

- [1] D. A. Babb, W. F. Richey, K. Clement, E. R. Peterson, A. P. Kennedy, Z. Jezic, L. D. Bratton, E. Lan, and D. J. Perettie, “Resin transfer molding process for composites,” 1998.
- [2] K. I. Tifkitsis and A. A. Skordos, “Real time uncertainty estimation in filling stage of resin transfer molding process,” *Polymer Composites*, vol. 41, no. 12, pp. 5387–5402, 2020.
- [3] S. Stieber, N. Schröter, A. Schiendorfer, A. Hoffmann, and W. Reif, “FlowFrontNet: Improving Carbon Composite Manufacturing with CNNs,” in *ECML PKDD*, 2021, pp. 411–426.
- [4] S. Stieber, A. Hoffmann, A. Schiendorfer, W. Reif, M. Beyrle, J. Faber, M. Richter, and M. Sause, “Towards Real-time Process Monitoring and Machine Learning for Manufacturing Composite Structures,” *ETFA - IEEE Emerging Technology and Factory Automation*, pp. 2–5, 2020.
- [5] B.-J. Wei, Y.-S. Chang, Y. Yao, and J. Fang, “Online estimation and monitoring of local permeability in resin transfer molding,” *Polymer Composites*, vol. 37, no. 4, pp. 1249–1258, 4 2016.
- [6] H. P. G. Darcy, *Les Fontaines publiques de la ville de Dijon*. V. Dalmont, 1856.
- [7] C. González and J. Fernández-León, “A Machine Learning Model to Detect Flow Disturbances during Manufacturing of Composites by Liquid Moulding,” *Journal of Composites Science*, vol. 4, no. 2, p. 71, 2020.
- [8] E. Fauster, D. C. Berg, D. Abliz, H. Grössing, D. Meiners, G. Ziegmann, and R. Schledjewski, “Image processing and data evaluation algorithms for reproducible optical in-plane permeability characterization by radial flow experiments,” *Journal of Composite Materials*, vol. 53, no. 1, pp. 45–63, 2019.
- [9] X. Shi, Z. Chen, H. Wang, D. Y. Yeung, W. K. Wong, and W. C. Woo, “Convolutional LSTM network: A machine learning approach for precipitation nowcasting,” in *Advances in Neural Information Processing Systems*, vol. 2015-Janua, 2015, pp. 802–810.
- [10] A. Vaswani, N. Shazeer, N. Parmar, J. Uszkoreit, L. Jones, A. N. Gomez, L. Kaiser, and I. Polosukhin, “Attention is all you need,” in *Advances in Neural Information Processing Systems*, vol. 2017-Decem, 6 2017, pp. 5999–6009.